Reactive and Functional Polymers 137 (2019) 27–37

Contents lists available at ScienceDirect

Reactive and Functional Polymers

journal homepage: www.elsevier.com/locate/react

Rheological modifiers based on supramolecular block copolymers: From weak associations to interconnected micelles

Hadi Goldansaz[a], Amir Jangizehi[b,c], Goolia Nikravan[b], Olivier Verkinderen[d], Bart Goderis[d], Seyed Reza Ghaffarian[b], Evelyne van Ruymbeke[a], Mostafa Ahmadi[b,c,*]

[a] Bio and Soft Matter, Institute of Condensed Matter and Nanosciences, Université Catholique de Louvain, Croix du Sud 1, B-1348 Louvain-la-Neuve, Belgium
[b] Department of Polymer Engineering and Color Technology, Amirkabir University of Technology, Hafez st. 424, Tehran, Iran
[c] Institute of Physical Chemistry, Johannes Gutenberg-Universität Mainz, Duesbergweg 10–14, 55128 Mainz, Germany
[d] Chemistry and Materials, Department of Chemistry, KU Leuven, Celestijnenlaan 200F, Box 2404, B-3001 Leuven, Belgium

ARTICLE INFO

Keywords:
Rheology
Supramolecular polymer
Tube-based model
Block copolymer
Morphology

ABSTRACT

The rheological spectra of poly(n-butyl acrylate) in the presence of a series of P(nBA-*b*-HEMA) rheology modifiers show a two-step relaxation process originating from the PnBA matrix and the self-assemblies. The HEMA segments are further grafted with strong, hydrogen bonding UPy groups, which both magnifies and slows down the relaxation of the assemblies. The extents of associations are enlightened by studying thermal transitions in DSC, morphological developments by SAXS, and description of rheological properties using a tube-based model. It is revealed that a weak association tendency, due to long hydrophobic blocks, leads to the formation of double-linear or star assemblies, while increasing the association strength results in the formation of micelles. In an optimum block length and UPy content, loosely entangled diblock additives can form an interconnected micellar network with significantly long relaxation time.

1. Introduction

The increasing complexity of daily life applications drives the need to synthesize and provide polymer materials with higher functionalities and enhanced properties. To address the current market requirements, material scientists should develop and introduce precursor materials on the basis of readily available chemistries, which can be largely tuned and modified to deliver the desired functionalities and specifications. This can be achieved by either assessing new materials and processes or using combinations of already existing ones in an entirely new and creative way. While the former strategy is time consuming and expensive to establish, the latter is appealing in terms of scientific achievement and applications. Examples of such methodology are abundant and typically include a "bottom–up" approach of thinking in a molecular design. An integrated part of this strategy is to successfully incorporate various chemical groups or molecules, which are typically incompatible, into a hierarchical assembly, which then synergistically delivers new functionalities and properties from the well-thought and balanced combination of chemical ingredients and physical interactions [1]. Supramolecular chemistry [2,3] therefore is a key in obtaining such fine-tailored hierarchy, especially when working with polymers in which chain connectivity tend to suppress their compatibility with additional building blocks, mainly because of entropic reasons.

Presently, the literature of associative polymers bearing strongly interactive, directional, stimuli-responsive, supramolecular motifs, such as ureido-pyrimidinone, terpyridine, or imidazoline is abundant [4–6]. There is a handful of synthesis strategies and well-architected libraries of supramolecular groups, which can be used to produce various sticky chain architectures with supramolecular motifs placed either along the polymer backbone or at chain extremities. Such supramolecular polymers often possess distinct viscoelastic features such as elevated elasticity, retarded terminal relaxation, complex time–temperature relationship, and significant nonlinear viscoelastic characters [7–10]. These features are partially understood and explained with regard to the formation of distinct microstructures by the weak binary or strong and highly directional collective assemblies of supramolecular motifs [8,9].

While the dynamics of polymer chains are well described by quantitative models in the light of the tube theory [11–13], the dynamics of supramolecular associations are not thoroughly predictable. The ideal picture from supramolecular systems is based on the "binary" association of stickers [7,14–16]; however, because of the difference in their chemistry and dynamics, they frequently form higher order structures known as "collective" assemblies [4,8,17]. For example,

* Corresponding author at: Department of Polymer Engineering and Color Technology, Amirkabir University of Technology, Hafez st. 424, Tehran, Iran.
E-mail address: mo.ahmadi@aut.ac.ir (M. Ahmadi).

https://doi.org/10.1016/j.reactfunctpolym.2019.01.008
Received 7 November 2018; Received in revised form 16 January 2019; Accepted 17 January 2019
Available online 29 January 2019
1381-5148/

simple hydrogen-bonding groups can phase separate into micro-domains, crystals, or stacks [4,18–23]. It has been recently reported that small hydrophobic substitutions can stabilize such micro-domains in an aqueous environment to generate strong hydrogels [24,25]. Metal ions in systems based on metal–ligand coordination or ionic interactions have also been reported to phase separate into clusters [26–31]. Owing to the higher stability of collective assemblies, such supramolecular systems show considerably slower dynamics, higher solid–liquid transition temperature, and, consequently, lower degrees of stimuli responsiveness [9,21,32,33]. Entangled polymer precursors are frequently avoided in the context of supramolecular systems because the complexity of chain dynamics combined with the binary and collective assembly of supramolecular motifs depreciates the description of the overall behavior and consequent material design [7,9,32], while such systems occur more frequently in practice.

The objective of the present work is to investigate how the presence of diblock copolymers, with the core being able to create supramolecular bonds, may affect the dynamics of polymer chains. The morphology and viscoelastic behavior of block copolymers, particularly the ones with immiscible blocks, have been investigated extensively [34–37]. It is well known that such macromolecular systems tend to phase separate in well-defined morphologies, spanning from cubic lattices to cylinders and lamellae, the details of which primarily depend on i) the volume fraction of the minor phase and ii) the demixing free energy having entropic contributions emerging from the relative block lengths and enthalpy terms originated from amphiphilic interactions (which can be seen as a nondirectional supramolecular interaction) among the blocks. The significance of such morphology is best seen by rheology in which cubic lattices lead to the formation of a second elastic plateau lower than that of the entangled network, while the bi-continuous cylindrical and lamellar phases are characterized by distinct slopes in the dynamic moduli against frequency [35]. In addition, disorder states may also occur when the immiscible blocks fail to form macro lattices but yet succeed to locally minimize the osmotic pressure through self-assembly.

Different soft matter systems based on a combination of block copolymers and modern supramolecular motifs have been designed and tested for various applications such as shock absorbers, nano-scafolding [38,39], and drug delivery [36,37]. For instance, Brassinne et al. synthesized a series of stimuli-responsive hydrogels made up of diblock copolymers bearing terpyridine groups at the extremity of the long block [40–44]. They illustrated that such macromolecules form 3D networks whose viscoelastic behavior is determined by the exchange timescale of the minor blocks among micelles, as well as the association/dissociation timescale of the terpyridine ligand-transition metal complexes. Similar combinations of diblock copolymers and strong, directional supramolecular associations have been utilized in bulk to create complex, responsive, and adaptive nanomaterials with well-defined morphologies used, for instance, in nanomembrane fabrication for selective metal depositions [38,39,45,46]. Most of these systems consist of two immiscible, covalently connected, asymmetric blocks, forming individual micelles or arrays, which are then self-assembled into a network through supramolecular groups placed at the free extremity of the long block. As expected, there are also a few contributions in which sticky groups are placed as side chains to the minor block [47–50]. For instance, the morphological phase behavior of block copolymers with ionic liquid groups such as imidazolium, pending from the minor block, is investigated in solutions [48] and in the melt state [47]. However, reports on viscoelastic properties of such copolymers across different regions of the phase diagram are less frequent.

Hence, in this work, we synthesize diblock copolymers in which self-complementary, hydrogen bonding, UPy motifs are grafted onto the short block, and this will presumably contribute to the properties of the minor phase. The volume fraction and surface tension between the two phases are varied by changing the length of the nonassociative block and varying UPy grafting density, respectively. The system consists of supramolecular block copolymers dispersed in a matrix of homopolymers with the same chemistry and length as those of the non-associative block. The evolution of rheology and microstructure and study of their relationship are our central focus. Our ultimate goal is to reach design guidelines for copolymer additives to modify the consistency of low viscosity polymers using strong supramolecular interactions, which promote the formation of an interconnected micelle network.

2. Experimental

2.1. Materials

2-(6-Isocyanatohexylaminocarbonylamino)-6-methyl-4[1H] pyrimidinone,UPy-hexyl-isocyanate, is synthesized as reported by Folmer et al. [51] n-Butyl acrylate and hydroxylethyl methacrylate are purified by passing through basic aluminum oxide. All other chemicals are purchased from Sigma-Aldrich and used without further purification.

2.2. Synthesis

2.2.1. Synthesis of poly(n-Butyl acrylate), PnBA, a macroinitiator

PnBA homopolymers, as a macroinitiator, are prepared by atom transfer radical polymerization (ATRP). In all polymerizations, the molar ratio of catalyst (copper bromide, Cu(I)Br):Ligand (N,N,N′,N″,N″-pentamethyl diethylene triamine, PMDETA) is 1. All macroinitiators are synthesized by the same general procedure, during which only the molar ratio of nBA:initiator (Ethyl 2-bromopionate, EBrP) is varied according to the targeted number-average molar mass. In a typical polymerization reaction (molar mass of 33 kg/mol), nBA (6 mL, 41.62 mmol) and PMDETA (14.61 μL, 0.07 mmol) are added to a 25 mL Schlenk flask. The mixture is degassed in three freeze–pump–thaw cycles. The catalyst (10.04 mg, 0.07 mmol) is added under N_2 atmosphere, and oxygen is removed by applying vacuum and back-filling with N_2 (3 cycles). These components are mixed at room temperature for 20 min for dissolving the catalyst and forming the catalyst–ligand complex. The flask is placed in a preheated oil bath at 60 °C, and an initiator (2.54 μL, 0.14 mmol) is added. After 24 h, the reaction mixture is diluted with 25 mL of tetrahydrofuran. The catalyst is removed by passing through basic alumina. The mixture is concentrated using a rotary evaporator, precipitated in cold methanol, and dried under vacuum. The relative (polystyrene-analog) number-average molar masses, M_n, and the polydispersity indices are determined by size-exclusion chromatography (SEC) (PSS-SDV 5 μL 1E3, 1E5, and 1E6 columns, 25 °C, tetrahydrofuran eluent, molar mass calibration with polystyrene standards). ^{1}H NMR ($CDCl_3$): δ = 4.06 (qq, OCH_2CH_2), 2.29 (m, CH_2CH in the polymer backbone), 1.92 (m, CH_2CH in the polymer backbone), 1.60 (m, $OCH_2CH_2CH_2$), 1.38 (m, $CH_2CH_2CH_3$), and 0.94 (m, $CH_2CH_2CH_3$) ppm.

2.2.2. Synthesis of poly(n-Butyl acrylate-b-hydroxyethyl acrylate), P(nBA-b-HEMA)

All block copolymers are synthesized by ATRP by the same procedure as described above, except that after the addition of a catalyst to the degassed mixture of HEMA and PMDETA, PnBA homopolymers are added to the mixture as macroinitiators. ^{1}H NMR ($CDCl_3$): δ = 4.06 (OCH_2CH_2), 3.8 (m, CH_2CH_2OH), 2.29 (m, CH_2CH in the polymer backbone), 1.92 (m, CH_2CH in the polymer backbone), 1.60 (m, $OCH_2CH_2CH_2$), 1.38 (m, $CH_2CH_2CH_3$), and 0.94 (m, $CH_2CH_2CH_3$) ppm.

2.2.3. Grafting of supramolecular moieties on the block copolymers, P(nBA-b-UPy)

Supramolecular polymers are obtained by functionalization of the P(nBA-*b*-HEMA) copolymers obtained in the previous step with UPy-hexyl-isocyanate. In a typical functionalization (Supramolecular polymer with a molar mass of 33 kg/mol, P(nBA33-*b*-UPy1)), P(nBA33-

b-HEMA) (1.7 g) is dissolved in 75 mL anhydrous toluene at 80 °C. UPy-hexyl-isocyanate, which is only partially soluble in toluene, (452.81 mg, 1.5 mmol) is added to the polymer solution. After specified grafting time (12 h for the case of P(nBA33-*b*-UPy1)), unreacted UPy-hexyl-isocyanate is removed by filtration. The product is precipitated in cold methanol, isolated by filtration, and then dried under vacuum. Different grafting times of 12 and 24 h were used to provide different levels of UPy content. ^{1}H NMR ($CDCl_3$): δ = 13.1 (s, CH_3CNH), 11.8 (s, $CH_2NHCONH$), 10.2 (s, $CH_2NHCONH$), 4.6 (s, $NHCOO$), 4.06 (OCH_2CH_2), 3.8 (m, CH_2CH_2OH), 3.2 (m, CH_2NHCOO, $CH_2NHCONH$), 2.29 (m, CH_2CH in the polymer backbone), 2.2 (s, CH_3CCH), 1.92 (m, CH_2CH in the polymer backbone), 1.60 (m, $OCH_2CH_2CH_2$), 1.38 (m, $CH_2CH_2CH_3$), and 0.94 (m, $CH_2CH_2CH_3$) ppm.

2.3. Characterization

Synthesis of UPy, monomer conversions, copolymer compositions, and UPy grafting on copolymers are determined by proton nuclear magnetic resonance (^{1}H NMR) spectroscopy. ^{1}H NMR spectra are recorded on a Bruker Avance 500 MHz spectrometer. Chemical shifts are reported downfield from tetramethylsilane in $CDCl_3$ or DMSO as a deuterated solvent at room temperature. Samples are annealed under vacuum at 90 °C for 1 day to equalize their thermal history before conducting viscoelastic and thermal studies. Thermal properties are studied by differential scanning calorimetry (DSC) on a Mettler-Toledo apparatus calibrated against indium and operating under nitrogen atmosphere. First, 10–15 mg of the dried sample is placed and sealed in a 40 μL aluminum pan and then cooled down to −90 °C at the rate of 10 °C/min. Glass transition temperature (T_g) of PnBA-based systems is determined during heating ramps from −90 to 100 °C at a rate of 10 °C/min. The experiment is repeated at least twice to ensure the reproducibility of the data. Glass transition temperatures were determined as the inflection point of the first-order thermal transitions.

Linear viscoelastic (LVE) responses of PnBA homo-, co-, and supramolecular polymers are measured in the frequency domain using 15, 8, and 4 mm parallel plate geometries of an MCR301 rheometer (Anton Paar, Germany). A fresh sample is loaded at 84 °C and then monitored for 15 min at a constant shearing amplitude and frequency (γ = 0.1–1%, ω = 1 rad·s^{-1}) to ensure sample equilibration. Next, a frequency sweep measurement is performed in the LVE regime. The sample is then cooled down step by step, equilibrated as described above, and measured down to −45 °C. Before frequency sweep experiments, LVE limit is determined at selected temperatures, i.e., 84, 30, and − 16 °C. The LVE limit at other temperatures is estimated from these values. For each selected temperature, the sample is first equilibrated at 84 °C, then cooled down, and equilibrated again at the desired temperature, and finally, an amplitude-sweep measurement is recorded at a constant frequency (γ = 0.1–100%, ω = 1 rad·s^{-1}) to determine the LVE regime.

Small-angle X-ray scattering (SAXS) measurements are conducted on a Xenocs Xeuss with a high-brilliance low-divergence Molybdenum source and a MAR345 image plate detector. Patterns are then converted to TIFF16 bit files using Fit2D [52] and subsequently azimuthally averaged using Conex [53]. Finally, background scattering is subtracted from the measured intensity of the samples, and data are plotted on double logarithmic scales.

3. Results and discussion

Self-assembly of supramolecular block copolymers has become an attractive topic because of the versatile morphological properties and potential applications [38,39,45,54]. It has been reported that the presence of supramolecular associative units can compete with the thermodynamic repulsion of phases and avoid/promote long-range macrophase separation [38,45]. In this work, this effect is further studied in supramolecular diblock copolymers by changing the length/weight fraction of the first block, as well as the fraction of supramolecular units incorporated in the second block. After a brief description of the synthesized samples, the evolution of rheological properties in three different sets of samples, namely, conventional, diblock, and supramolecular diblock copolymers, at two levels of UPy content is presented and correlated with microstructural specificities deduced from SAXS measurements.

3.1. Synthesis and characterization

Three sets of samples are synthesized, for which the number-average molar mass (M_n) of nonassociative PnBA block is changed from 8 to 33 and 81 kg/mol. Considering the entanglement molar mass of PnBA [7,9], these samples cover the range of non- to well-entangled chains. All samples are connected to the HEMA block with relatively constant length (fixed by the molar ratio of monomer to macroinitiator). The appearance of a low molar mass shoulder due to the presence of unreacted macroinitiators in a two-step ATRP approach for the synthesis of diblock copolymers has been frequently reported [55–57]. Such imperfection could be avoided by the application of higher reaction times in the second ATRP step or halogen exchange strategy [55,57,58], or utilization of one-pot synthesis through the successive addition of monomers [59]. However, following our industrial purpose, it could be regarded as an advantage for the specific target of having only a small fraction of diblock chains as rheology modifiers. Therefore, our samples can be regarded as a mixture of P(nBA-*b*-HEMA) block copolymers in PnBA chains, where the length of the PnBA block is the same as that in the matrix.

The HEMA blocks are subsequently functionalized by the strong self-complementary UPy motifs at different reaction times, which yielded approximately 25 and 50 mol% of UPy functionalization in the HEMA block. The molecular characteristics of the synthesized copolymers are described in Table 1.

Block copolymers are represented by P(nBAx-*b*-HEMA) codes, where x denotes the M_n of the first PnBA block, and supramolecular systems are signified by P(nBAx-*b*-UPyz), where the UPy grafting times of the second block, corresponding to 12 and 24 h, are denoted by z numbers of 1 and 2, respectively. The chemical structure and ^{1}H NMR spectra of the representative block copolymer and supramolecular copolymer and the corresponding peak assignments are shown in Supporting Information (Fig. S1).

The combined SEC and ^{1}H NMR measurement results, reported in Table 1, reveal that samples have an almost comparable length of HEMA blocks. However, ^{1}H NMR data reflect the average bulk properties and provide no information about the exact distribution of block lengths. Additionally, the absolute quantities might be deceptive because, generally, in a dilute solution, the NMR signals of a particular atom is considered to be solely coupled to the neighboring atoms residing on the same chain, whereas in the case of a strongly associative copolymer, the signals must have contributions from coupling among the neighboring chains, which could be in close proximity due to the self-assembly of associative HEMA or UPy units. Such effect makes the quantification of ^{1}H NMR data in these systems rather challenging.

The distributions of molar masses (MMDs) before and after the growth of the second block are compared in Fig. 1. A higher molar mass shoulder appears after the second ATRP step at shorter elution times, which reflects the fraction of diblock copolymers. This fraction could be increased upon an increase in reaction time or application of the halogen exchange strategy; however, it contradicts our target of having a short hydrophilic block. Weighted summation of two log-normal distributions is used to deconvolute the contribution of high molar mass shoulder, and the results are depicted in Fig. 1. Within 5% error, all samples have approximately 25% of diblock copolymers. Consequently, on the basis of the combined SEC and ^{1}H NMR results, the systems could be viewed as comparable mixtures of self-assembled block copolymers in a large matrix of homopolymers where the length of the

Table 1
The molecular characteristics of the synthesized block copolymers and supramolecular systems.

Sample	Homopolymer		Diblock copolymer				T_g (°C)
	M_n (kg/mol)	PDI	wt%[a]	$DP_{HEMA\ block}$[b]	DP_{total}	(UPy/HEMA) (mol%)[c]	
PnBA8	7.6	1.4	–	–	59	–	−52
P(nBA8-*b*-HEMA)	–	–	21	96	155	–	−51.2
P(nBA8-*b*-UPy1)	–	–	nd	96	155	25	−54.5
PnBA33	33.2	1.3	–	–	259	–	−49
P(nBA33-*b*-HEMA)	–	–	30	73	332	–	−49.5
P(nBA33-*b*-UPy1)	–	–	nd	73	332	22	−51
P(nBA33-*b*-UPy2)	–	–	nd	73	332	50	−51.5
PnBA81	81.1	1.2	–	–	633	–	−50
P(nBA81-*b*-HEMA)	–	–	24	104	737	–	−50
P(nBA81-*b*-UPy1)	–	–	nd	104	737	23	−58
P(nBA81-*b*-UPy2)	–	–	nd	104	737	45	−62.5

[a] Calculated from the deconvolution of SEC curves (see Fig. 1).
[b] Calculated from SEC and ^{1}H NMR data.
[c] Calculated from ^{1}H NMR data.

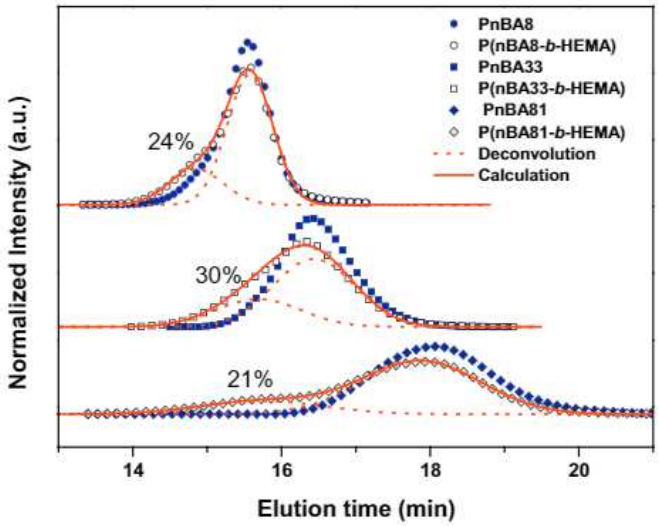

Fig. 1. Molar mass distribution of the PnBA precursors and the corresponding block copolymers. Dotted lines denote deconvolution to Gaussian distributions and dashed lines denote their weighted summation. Numbers denote the fraction of shoulders at lower elution times.

first block and matrix chains are systematically varied. Such systems are similar to the mixture of homo and block copolymers studied by Watanabe et al. [60,61].

3.2. Rheological properties in the presence of traditional diblock copolymers

Rheological properties are very sensitive to microstructure and have been extensively used as an indirect method for better analysis of the synthesized polymers [62,63]. Fig. 2a shows the isofriction mastercurves of storage moduli of the PnBA precursors. As expected, the unentangled PnBA8 sample displays a Rouse-like relaxation while the terminal regime is achieved for entangled PnBA33 and PnBA81 after a plateau modulus that extends further for larger average molar mass. These data are compared to the corresponding storage moduli of the diblock samples. Both P(nBA8-*b*-HEMA) and P(nBA33-*b*-HEMA) show an additional low frequency relaxation process. The effect of the second block on the rheological properties of P(nBA81-*b*-HEMA) is less pronounced and is mainly manifested by negligible prolongation of the final relaxation than the corresponding precursor. We can accordingly divide the spectrum in high-, medium-, and low-frequency regions, respectively; where there is no difference in the relaxation of the matrix chains and rheology modifiers, the matrix chains disentangle and the diblock copolymers can perform their terminal relaxation.

A similar behavior has been frequently reported for binary blends of linear chains, when the reptation times of two components are well separated [64]. In such case, the low-frequency relaxation time and moduli can be used to determine the length and fraction of longer chains, respectively. However, here, the hydrophobic HEMA segments of diblock fractions have the potential to phase separate into micelles and to create larger assemblies. Previous studies on similar diblock systems, dispersed in an unentangled matrix, have shown that such phase-separated micelles can relax by Brownian motion across a distance approximately equal to the core diameter [60,61]. Neglecting the polydispersity, a similar behavior could be expected from the PnBA8 sample series. However, the other two sample series include entangled chains that hinder the Brownian motion of phase-separated units.

The relaxation time of the block copolymers can be better analyzed by removing the contribution from the relaxation of the matrix chains. For this purpose, the terminal relaxation times of the three homopolymers are matched by horizontally shifting and overlapping the dynamic moduli in the terminal region of PnBA33 and PnBA8 to that of PnBA81, as shown in Fig. 2b. Then, the same horizontal shift factors are applied to the dynamic moduli of P(nBA33-*b*-HEMA) and P(nBA8-*b*-HEMA) to exclude the contribution of the PnBA matrix to the viscoelastic spectra. The results are also shown in Fig. 2b in which the difference between the apparent normalized terminal relaxation times addresses the extent of self-assembly in the systems. It is apparent that the block copolymers have slower relaxation than the PnBA homopolymers in all series. Relaxation time increases from P(nBA8-*b*-HEMA) to P(nBA33-*b*-HEMA) as a direct effect of entanglement; however, it decreases upon further increase in the PnBA block length. The inherent dilution effect of longer soft chains in P(nBA81-*b*-HEMA) prevents effective self-assembly of these copolymers, and thus, the micelle relaxation is barely visible in this sample. In other words, the strongly reduced volume fraction of the HEMA block in P(nBA81-*b*-HEMA), as compared to the other samples, prevents their effective assembly.

3.3. Rheological properties in the presence of supramolecular diblock copolymers

Diblock copolymers were grafted with UPy motifs at two different reaction times. The resulting supramolecular diblock copolymers are therefore expected to possess relatively medium and high UPy contents. The heterogeneity in the distribution of block length is expected to be further amplified due to the variation in the number of UPy motifs per chain caused by the random nature of the grafting reaction. The isofriction mastercurves of PnBA precursors, diblock copolymers, and corresponding supramolecular copolymers with a medium UPy content,

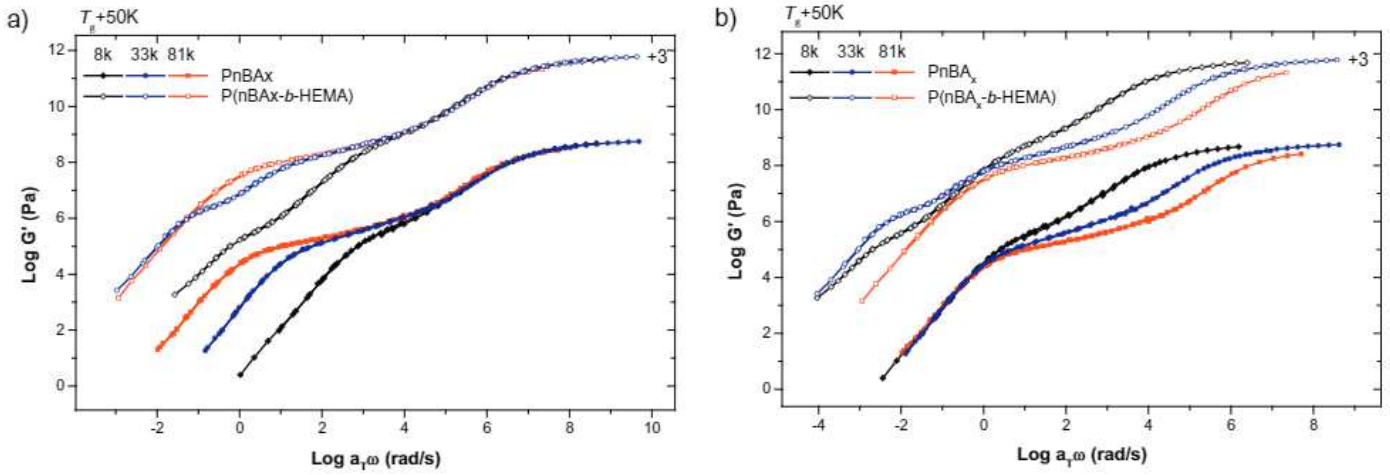

Fig. 2. Storage moduli of (a) PnBA homopolymers and blends with diblock copolymers, (b) PnBA8 and PnBA33 are shifted horizontally to overlay PnBA81 at the terminal zone, and the same shift factor is applied to P(nBA8-*b*-HEMA) and P(nBA33-*b*-HEMA) to remove the effect of the PnBA matrix on the terminal relaxation. P (nBA-*b*-HEMA) curves are vertically shifted by 3 orders of magnitude for better visualization.

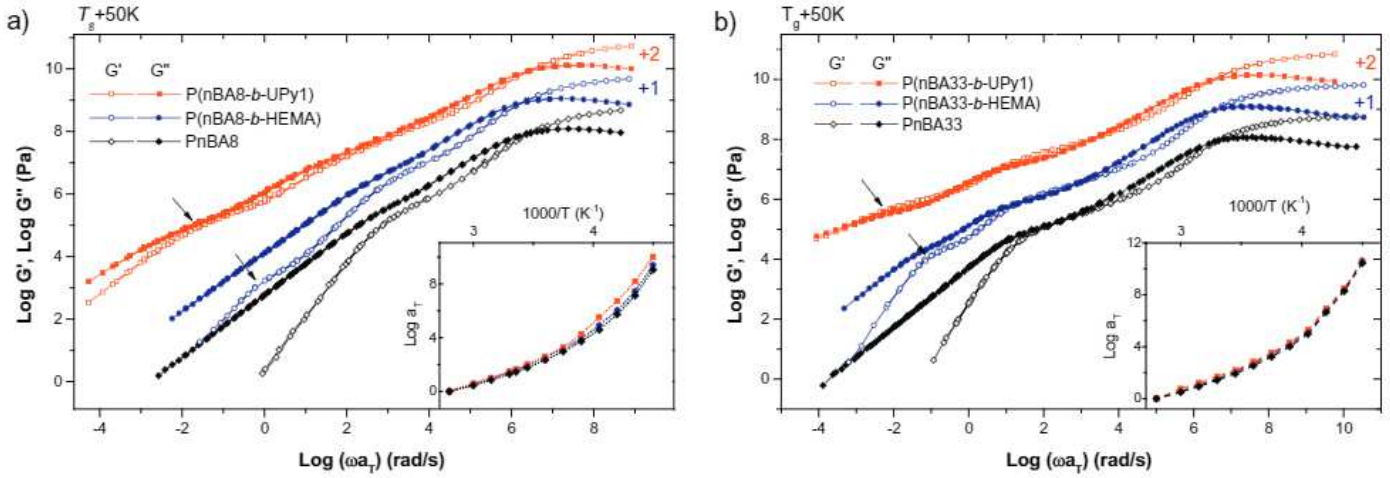

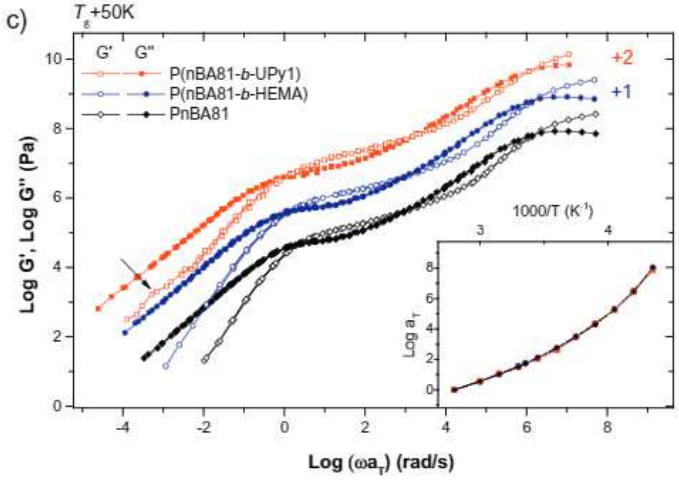

Fig. 3. Dynamic moduli of PnBA homopolymers and blends with diblock and supramolecular copolymers: (a) PnBA8 series, (b) PnBA33 series, (c) PnBA81 series (main plots), and corresponding shift factors (inset plots). As indicated by arrows, while the presence of diblock and supramolecular chains is distinguishable as the second relaxation in lower frequencies for PnBA8 and PnBA33 series, it is only reflected as a shoulder in loss modulus of P(nBA81-*b*-UPy1) in PnBA81 series. The P (nBA-*b*-HEMA) and P(nBA-*b*-UPy) curves are vertically shifted by 1 and 2 orders of magnitude, respectively, for better distinction.

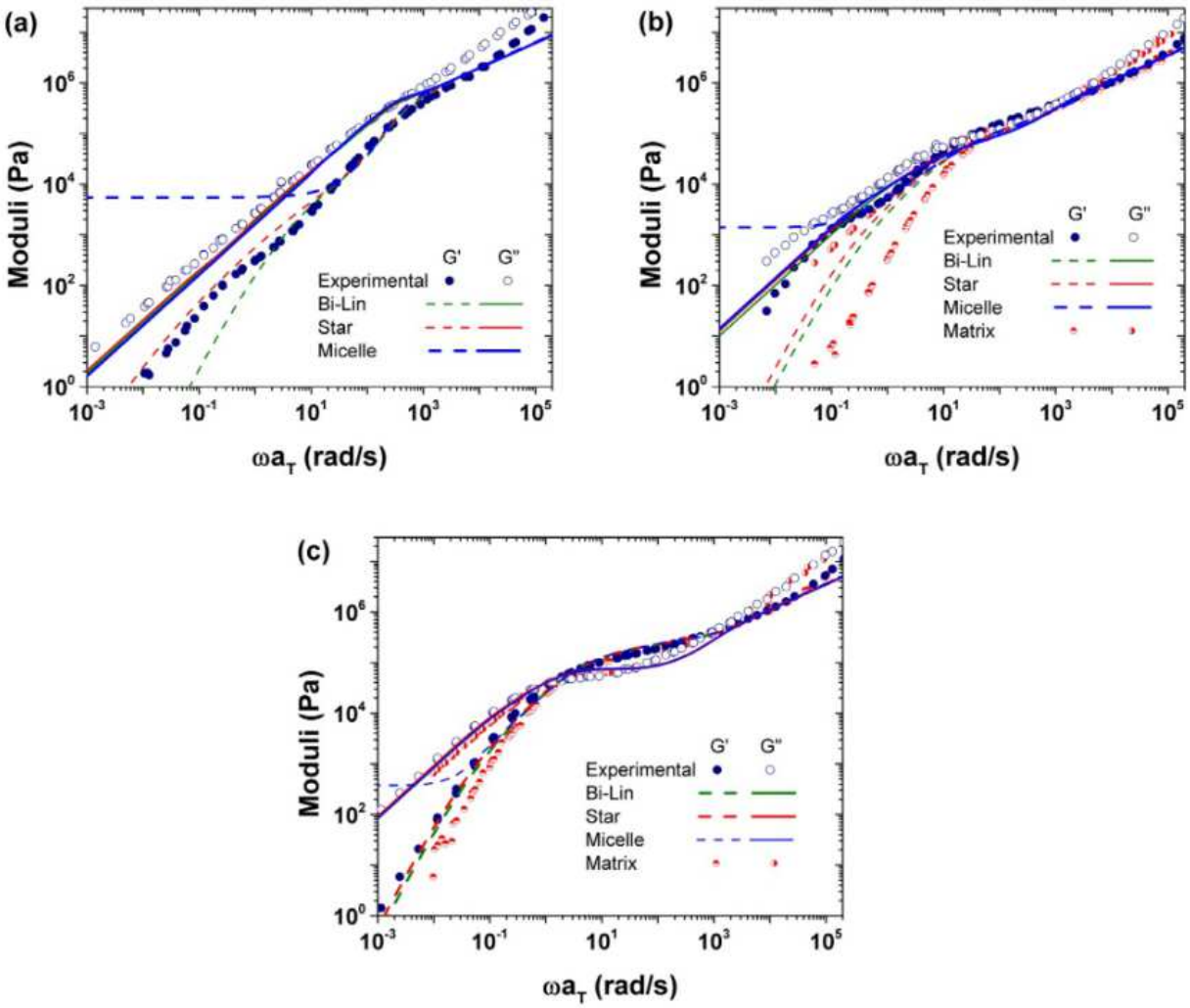

Fig. 4. Comparison between model predictions and experimental dynamic moduli of the (a) P(nBA8-*b*-HEMA), (b) P(nBA33-*b*-HEMA), and (c) P(nBA81-*b*-HEMA), blended to the linear matrix (weight fractions are given in Table 1).

as well as the corresponding shift factors, are compared in Fig. 3.

It is observed that the rheological behaviors of samples are extensively altered across the frequency axis after grafting with UPy motifs. The higher frequency relaxation process originates from the PnBA matrix, and the second relaxation process results from the self-assemblies. The relaxation of self-assemblies are both magnified and slowed down in the presence of supramolecular motifs, thus suggesting the formation of higher order assemblies. For the case of the PnBA81 series, the process of phase separation and creation of assemblies only appears in the presence of UPy motifs, as a low-frequency shoulder in storage modulus. However, it is clear that the effect of adding supramolecular bonds is much more pronounced for copolymers with shorter nonassociative blocks.

The corresponding horizontal shift factors for the construction of master curves of the PnBA precursor, diblock copolymers, and supramolecular block copolymers are compared in the inset plots of Fig. 3. It is important to note that no vertical shift is used in reducing the data to the mastercurves (except for the vertical shifts exerted for a better distinction of the curves), which means that the samples do not show any first-order thermal transitions. All samples exhibit WLF-like flow behavior. Addition of a hydrophilic block and supramolecular moieties does not significantly alter the overall shift factors for samples attached to the PnBA block longer than the entanglement length. In other words, it is still the relaxation of entangled PnBA chains that dominates the flow behavior even at low frequencies. Conversely, the PnBA8 sample exposes larger shift factors and higher activation energies at higher temperatures, when the HEMA segment is added and even more strongly when the supramolecular bonds are introduced. It could be concluded that the dynamics of the unentangled PnBA segment is already exhausted at such temperatures, and only collective assemblies determine the flow behavior at this regime, which becomes more resistant to flow upon addition of stronger hydrogen bonds. In conclusion, increasing the length of the hydrophobic block, i.e., reducing the volume fraction of the HEMA segments, decreases the segregation affinity of the hydrophilic block. However, increasing the association tendency of hydrophilic blocks by the introduction of strong supramolecular motifs can promote self-assembly.

3.4. Insights from modeling

The exact microstructure formed in the presence of HEMA blocks and UPy motifs can be further illuminated in the light of a quantitative tube-based model. Three scenarios can be suggested according to the experimental data presented thus far. A weak association tendency can form linear chains with twice the length through an end-to-end linkage of block copolymers. Such system can then be regarded as a binary blend composed of the linear matrix and the double-linear chains, both relaxing by normal reptation and contour length fluctuations (CLF) according to the tube model. An increased association can even create star-like assemblies through an end-to-end linkage of more than two

block copolymers. Such system can be dealt as a binary blend of linear matrix and star chains, while star components relax only by CLF. Finally, a very strong association affinity can lead to the formation of micelles with a hard core. In such system, the corona, with the same molar mass as that of the matrix, can relax only by CLF, while the core relaxation can only take place at longer times, either by Brownian motion, governed by the motion of the polymeric fraction, or by disassembly of the core, at specific time which cannot be predicted by tube-based models.

A general tube-based model is developed according to the Time-Marching Algorithm (TMA) to test the suggested relaxation scenarios. Details of model development are further described in the Supporting Information and can be found elsewhere [13,65]. The general TMA model is first compared to the experimental moduli data of PnBA33 and PnBA81 and fitted to obtain the model parameters including entanglement molar mass (M_e), plateau modulus (G_N^0), and Rouse relaxation time of an entanglement segment (τ_e) [65]. The experimental data of PnBA8 is not included because such sample is expected to fully relax by the Rouse mechanism. The obtained results are depicted in Fig. S2.

The model is further updated to include the contribution of block and supramolecular copolymers in the dynamic moduli according to the suggested scenarios. Rheology modifiers are first considered to form linear chains with double length through weak associations. Such associations, formed by quadruple hydrogen bonding motifs, are expected to be strong enough that the formed double chains can relax by common polymer dynamics before the physical linkages dissociate. Consequently, the system should be viewed as a binary blend of linear chains (i.e., the matrix) and double linear chains (i.e., the associated copolymers). The proportion of the copolymers in different samples is reported in Table 1, and in the model, they have been all considered as participating to double-linear chains. The corresponding results coded as “Bi-Lin" are shown by green lines in Figs. 4 and S3 for block and supramolecular copolymers, respectively. The predictions obtained by considering that the rheology modifiers form star chains through stronger associations are also presented as red lines and coded as “Star.” The difference with the former scenario is that the star components are incapable of reptation and further prolong the final relaxation. Finally, rheology modifiers are considered as micelles, where the polar blocks make a hard core, whose relaxation is neglected in the current model. The only relaxing part of the block copolymers are the PnBA blocks, which form the corona. Their relaxation is slower than that of the PnBA matrix, as they are incapable of reptation, yet faster than the stars, considered in the former scenario, due to shorter arm length. Predictions are expected to deviate from the experimental data at the low-frequency region, as cores take time to relax. In the model, they are considered to be permanent, and no guess is made for their equivalent lifetime. The corresponding predictions coded as “Micelle” are presented as blue curves in Figs. 4 and S3 for block and supramolecular copolymers, respectively.

It must be noted that the main difference in the model for the determination of the relaxation moduli of the block (see Fig. 4) and the supramolecular (see Fig. S3) copolymers is the weight fraction of polar blocks, which should be updated according to the number of UPy motifs present in supramolecular systems. The effect of UPy stickers on the lifetime of associations are accordingly neglected, as copolymers are considered to relax by polymer dynamics before associations may open. It is worth mentioning that the modeling based on neglecting any kind of associations (Unimer model) provided results very close to the matrix behavior and are therefore neglected.

As shown in Fig. 4c, the behavior of P(nBA81-*b*-HEMA) is well captured by both Bi-Lin and Star models. The overlay of Bi-Lin and Star model predictions shows that rheology modifiers relax mainly by fluctuations. The reason is that while fluctuations can immediately use the already-relaxed matrix chains to dilate the tube (according to the dynamic dilution mechanism) and accelerate the relaxation, reptation has a time-lag to take this advantage (according to Graessley's criteria), and therefore, most of the associated star or double-linear chains will relax by the CLF mechanism [65,66]. The length of the hydrophilic block in this sample is only ~16% of the hydrophobic block (see Table 1), and in the binary associated state, they form chains almost twice the length of the matrix chains, and therefore, their influence can be well captured by the simple Bi-Lin model.

Both the Bi-Lin and Star models are too fast for the P(nBA33-*b*-HEMA) sample (Fig. 4b). In this case, the length of the second block is ~28% of the first block, and compared to the matrix (prediction curves compared to the red circles), such increase in length (e.g., ~2.5 times in binary association) has an influential effect. However, this is not enough, and the experimental data demonstrate even higher orders of association. Interestingly, the Star model can nicely reproduce the behavior of the P(nBA8-*b*-HEMA) sample (Fig. 4a). As reported in Table 1, the second block is more than 1.6 times the length of the first block, and in the associated state, they lead to chains with more than 5 times the length of the matrix, which has a significantly longer fluctuation time, as comprehended through the low-frequency relaxation step. The dilution due to the presence of almost 75% of the already-relaxed matrix cannot help fluctuations to overtake reptation, and therefore, the prediction by the Star model shows a significant difference, compared to Bi-Lin predictions.

For P(nBA8-*b*-HEMA) and P(nBA33-*b*-HEMA), we can also attribute the extra relaxation shoulder observed in the experimental data to the influence of micellar structures. With the Micelle model, the data are indeed well described at high and intermediate frequencies but show a low-frequency plateau due to the presence of the permanent core of the micelles.

Thus, the obtained results clearly show that weak association tendencies in rheology modifiers with long hydrophobic blocks can form double-linear or star chains, while decreasing the corresponding block length increases association strength and leads to micellar assemblies.

Interestingly enough, modeling results on supramolecular systems, depicted in Fig. S3, reveal that both Bi-Lin and Star scenarios produce too fast relaxations in all cases. The Micelle model can only reproduce the experimental behavior of P(nBA81-*b*-UPy) at intermediate frequencies, and it is yet too fast for the other samples. Thus, in the case of polymers involving rheology modifiers based on supramolecular assemblies, even the relaxation of matrix chains are affected and slowed down in the presence of supramolecular motifs. The origin of such interactions is not definitive, but it should be due to either the increased friction or higher topological constraints against polymeric dynamics. The presence of unassociated UPy groups in bulk, as discussed in Section 3.6, may lead to higher friction, and the presence of a higher fraction of relatively nonrelaxing supramolecular assemblies may increase the constraints and decrease the effective dynamic dilution for the relaxation of matrix chains.

3.5. Effect of UPy content

The samples P(nBA33-*b*-HEMA) and P(nBA81-*b*-HEMA) were grafted with UPy motifs for longer reaction times to study the effect of higher UPy contents. Two remarkably different behaviors are observed in corresponding dynamic moduli as depicted in isotemperature mastercurves in Fig. 5. P(nBA33-*b*-HEMA), in which the hard/soft block ratio is large enough to enable effective micellization, undergoes significant network formation by increasing the UPy content on its hard block. At medium UPy concentration, P(nBA33-*b*-UPy1), multiple elastic plateaus and relaxation processes are observed, while at high UPy grafting density, P(nBA33-*b*-UPy2), a very broad and elastic plateau is seen throughout the frequency axis with two orders of magnitude higher elasticity than the rubber plateau of entangled PnBA. Consequently, chain relaxation in the hypothetical tube formed by the lateral entanglements with neighboring chains is no longer valid. Such high elastic plateau in the P(nBA33-*b*-UPy2) sample suggests the

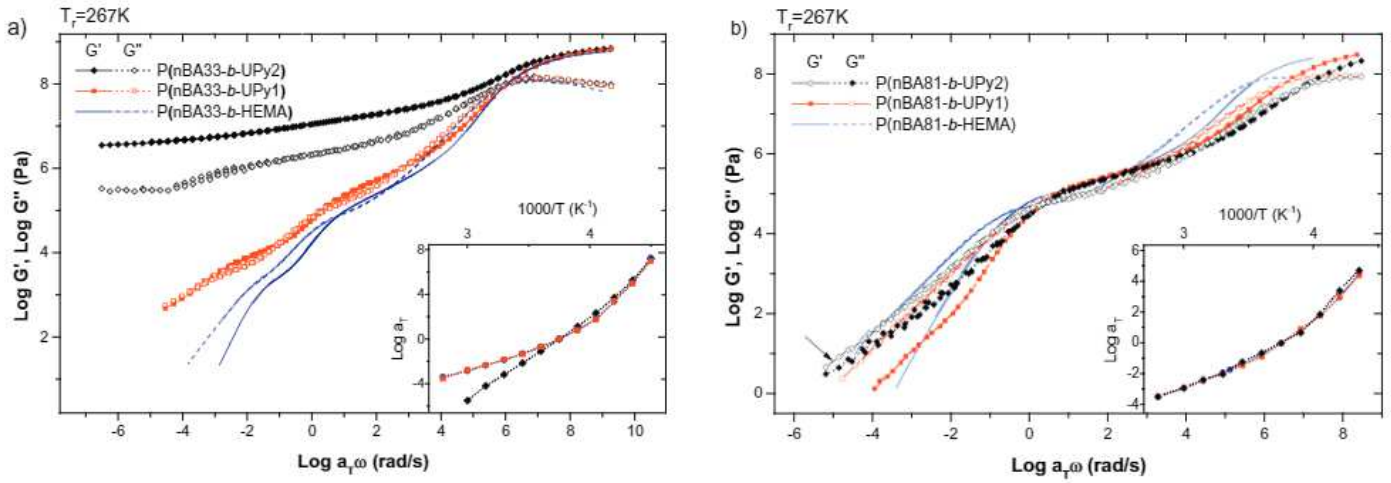

Fig. 5. Effect of UPy content on the dynamic moduli of (a) PnBA33 series (b) PnBA81 series (main plot) and corresponding shift factors (inset plot). Although the formation of interconnected micellar network is recognized by a large plateau in P(nBA33-*b*-UPy2), the dynamic moduli of P(nBA81-*b*-UPy2) only tend to show a low frequency plateau (indicated by an arrow) that imply the possible formation of a weak network.

presence of a percolated network with very large or no terminal relaxation time through which the stress is sustained. The presence of new percolated constraints, hindering chain dynamics, is further discussed according to SAXS results. Network formation in this sample is accompanied by huge deviation of the shift factors from that of PnBA and some visible thermorheological complexities at intermediate frequencies. On the contrary, in the PnBA81 series, where the probability to find chain-ends is evidently small and thus micelle formation is hampered, as demonstrated by TMA modeling, neither a network formation nor an alteration of viscoelastic shift factors are observed even at higher UPy contents. Only a low frequency, low magnitude semi-elastic plateau is detectable in P(nBA81-*b*-UPy2). The dominant viscoelastic feature in these samples is a strong alteration of the glass transition (see the last column of Table 1) and acceleration of Rouse relaxation time that eventually results in a faster departure from the rubber plateau at isotemperature, along with broadening of this elastic plateau upon UPy grafting.

3.6. Insights from morphological studies

Glass transition temperatures of the PnBA precursor and corresponding diblock systems are listed in Table 1. Interestingly, only one T_g, corresponding to the PnBA block (approximately −50 °C), could be recognized in all samples. In contrast to most of the former reports on the polyacrylates randomly grafted with UPy, in which T_g increases by 4–5 °C for every mol% of UPy [10,67], in the current P(nBA-*b*-UPy) systems, T_g decreases with an increase in the UPy content. Note that the results have been successfully reproduced after multiple purification and extensive drying steps of the samples to exclude any effect of residual solvent or impurities on the glass transition process. Furthermore, T_g decreases faster in the PnBA81 series where micelle formation is undermined by the lower concentration of chain ends than other series. This suggests that in the P(nBA81-*b*-UPy) series, a larger fraction of hard blocks and, consequently, UPy groups are accommodated in the matrix rather than being separated into the micelle cores. Thus, one can expect that the massive volume of UPy groups floating in the PnBA matrix can alter the packing length of this phase. In other words, decreasing the glass transition temperature could be correlated with an increase in free volume due to the presence of bulky UPy moieties residing in the PnBA phase.

Alteration in the molecular packing length is examined by investigating interchain distance by X-ray scattering. Two distinct peaks are observed in the room temperature diffractogram of supramolecular and diblock copolymers shown in Fig. 6. The strong, sharp peak at 1.25

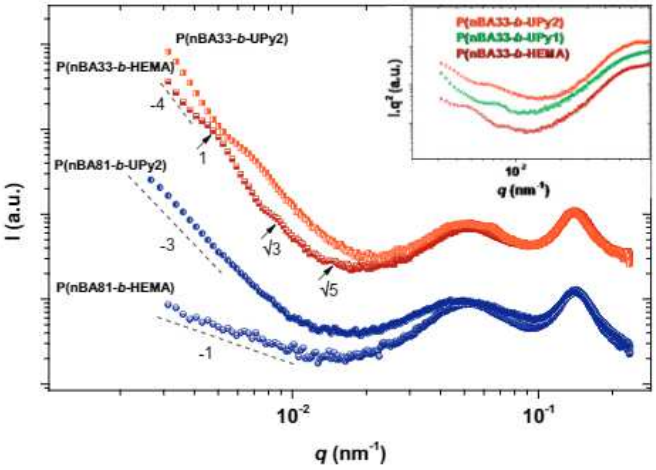

Fig. 6. Double logarithmic plot of SAXS intensity, I(q) (main plot) and Kratky plot $I(q)q^2$, against the magnitude of scattering vector (inset plots). Curves are vertically shifted for better distinction.

(A^{-1}) is reportedly assigned to the holes between successive side groups of acrylic monomers [68,69], whereas the relatively broad diffraction one at approximately 0.5 (A^{-1}) reflects the spacing between the adjacent chains in the PnBA phase [68]. Beiner and Huth demonstrated that the position and intensity of the former diffraction is very sensitive to the chemical composition of poly(n-alkyl acrylates), for instance, by increasing alkyl chain length, this peaks shifts to lower q positions.[51] The first diffraction peak at 1.25 (A^{-1}) in Fig. 6 does not change in any of the samples, as the side chain spacing in both acrylate and methacrylate blocks is identical and approximately 2C—C bonds. This observation rules out the possibility of undesired hydrolysis of the PnBA block during the grafting reaction. The 0.5 (A^{-1}) peak, which represents interchain distances in the PnBA phase, widens up in P(nBA81-*b*-HEMA) upon UPy grafting, thus confirming the increase in the packing length of this phase. Contrary to the high molar mass samples, P(nBA33-*b*-UPy2) only shows minor deviation in the left flank of the 0.5 (A^{-1}) peak and therefore no significant alteration in packing density. Hence, the glass transition in P(nBA33-*b*-UPy2) is expected to be only marginally smaller than that of the diblock precursor. The decreasing trend observed in chain spacing, which is in line with rheology and DSC results, confirms our argument that the unassociated UPy motifs, accommodated in the PnBA phase either due to failure in phase

separation or as the natural consequence of thermodynamic equilibrium between the two phases, are responsible for the decrease in T_g. The higher the concentration of UPy in the PnBA phase, the higher the interchain spacing and the lower the T_g.

The upturn in the scattering vector below 0.1 (A^{-1}) together with the emergence of a number of diffraction peaks (further highlighted in the Kratky representation in the insert plot) arises from the interaction of X-ray with micelles. In P(nBA33-*b*-HEMA), three broad and partly convoluted diffraction peaks with 1, $3^{1/2}$, and $5^{1/2}$ spacing are observed, which may suggest a disorder bcc lattice [70]. In supramolecular copolymer counterparts, a steeper upturn with a very broad peak as a shoulder reflects larger but highly polydisperse micelles. The slope of -4 suggests the presence of scattering objects of various sizes and shapes that are too big to be resolved in the corresponding scattering angle. Additionally, the broadening and gradual shift of these shoulder peaks toward lower q also implies polymorph micellar formation with a wide size distribution, which is promoted by an increase in volume fraction and tendency of the HEMA block to phase separate. Considering the multiplicity of the scattering objects and the dispersity in their shape and size, and with regard to the quality and extent of experimental data, using any simple scattering model could be an ill practice. Therefore, we limit our discussion to the impact of UPy functionalization on the chain packing and its correlation with T_g (WAXS region).

A general view can be developed from the explained rheological measurements and scattering data. Fig. 7 illustrates the morphological development in the studied sample series upon increasing the length of the PnBA block. According to the SAXS and rheological measurements, block copolymers form a perceptible phase-segregated structure. Increasing the length of the nonpolar PnBA block decreases the association tendency so that the PnBA81 series can mainly form double-linear and star associations. The micellar structures can most probably diffuse and relax by Brownian motion; otherwise, if the matrix and corona are not entangled, they can form an interconnected entangled network (see Fig. 7b and c), which diminishes after disassembly of cores or the slow diffusion through cage breaking. On the other hand, the size and dispersity of phase-segregated domains increase by adding strong hydrogen bonding UPy motifs. The stress carried by this interconnected network results in a high elastic plateau ($\sim 10^7$ Pa) as observed in Fig. 5. Nonetheless, this network possesses a small yield stress, as it can be easily scraped and shaped. In the absence of any external stress field, the sample retains its shape for months, thus confirming the observed rheological data, in which no terminal behavior is observed. Consequently, by promoting the phase separation of minor blocks by bulky supramolecular groups, it is possible to tailor the viscoelasticity and morphology of polymer melts and create highly elastic, yet brittle networks.

4. Conclusions

Following an industrial approach, blends of amphiphilic poly(n-butyl acrylate-*b*-hydroxyethyl methacrylate), P(nBA-*b*-HEMA) block copolymer, and poly(n-butyl acrylate), PnBA, have been synthesized in situ by a two-step ATRP method. The block copolymer fraction can be therefore considered as rheology modifiers in the PnBA matrix. The length of HEMA segments were kept constant in all samples, and the length of PnBA blocks were systematically increased from unentangled to well entangled. The effect of increasing levels of grafting 2-ureido-4[1H]-pyrimidinone (UPy) motifs on HEMA segments has also been studied. Rheological data confirm different levels of self-assemblies through the appearance of low-frequency relaxation steps. Further tube-based modeling efforts revealed that long PnBA blocks can decrease association tendency and lead to the formation of double-linear or star chains, whereas short hydrophobic segments can promote the formation of micellar assemblies.

UPy functionalization has a complex effect on both dynamics and microstructure. In unentangled and loosely entangled PnBA systems, grafting HEMA blocks with UPy units increases the micelle volume fraction and broadens their size and shape distribution, as evidenced in SAXS. A huge retardation of terminal relaxation time and emergence of other slow relaxation processes beyond that of the matrix chain was noticeable. Eventually, at high UPy coverage of the core, a highly elastic but brittle network was formed with an extended rubbery plateau modulus that was several orders of magnitude higher than that of entangled PnBA. Retardation of terminal relaxation time was accompanied by an abrupt change in the flow activation energy. This is believed to be the result of a percolated, 3D network of micelles that sustain the stress alongside with the soft PnBA phase. On the other hand, in the well-entangled PnBA block, UPy functionalization did not lead to effective micellization due to the intrinsic dilution effect of the PnBA phase. Scattering results demonstrated that the interchain packing density of the PnBA phase has decreased. This correlates with a sharp decrease in T_g, measured by both rheology and calorimetry, which is presumably due to the large fraction of bulky UPy groups, unable to phase separate, and hence residing in the matrix. Overall, the results exhibit the possibility of engineering rheology of low-viscosity polymers by employing diblock copolymers bearing bulky supramolecular groups along the minor block. Albeit, the success of this scenario depends on the right compromise between corona length and core functionalization, thus allowing us to take advantage of both entangled matrix and percolated micellar networks.

Acknowledgment

This work has been partly supported by the E.U. (Marie Sklodowska-Curie ITN “Supolen,” no. 607937), as well as Iran's National Elites Foundation. HG and EvR are Research Associates of FRS-FNRS. M. Ahmadi is a Georg Forster fellow of the Alexander von Humboldt foundation and gratefully acknowledges this support.

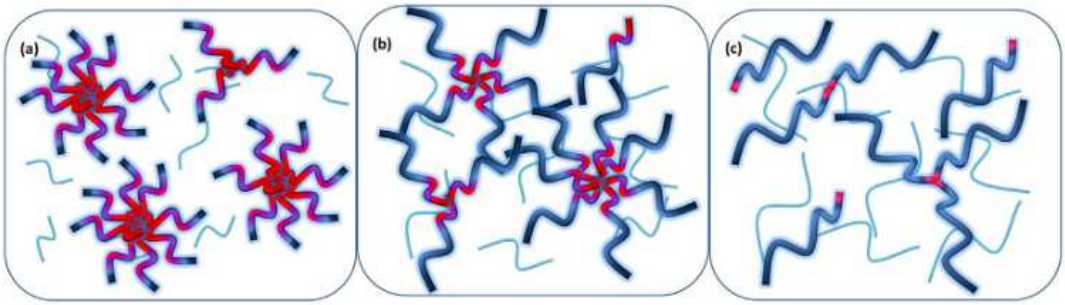

Fig. 7. Development of the morphology of phase-separated block copolymers: (a) independent micelles in nonentangled systems, (b) mixtures of micelles and lower levels of association forming an interconnected network and (c) lower levels of association in the presence of long nonpolar blocks.

Appendix A. Supplementary data

Supplementary data to this article can be found online at https://doi.org/10.1016/j.reactfunctpolym.2019.01.008.

References

[1] G.M. Whitesides, J.P. Mathias, C.T. Seto, Molecular self-assembly and nanochemistry: a chemical strategy for the synthesis of nanostructures, Science 254 (5036) (1991) 1312–1319.
[2] T. Aida, E. Meijer, S. Stupp, Functional supramolecular polymers, Science 335 (6070) (2012) 813–817.
[3] S. Seiffert, J. Sprakel, Physical chemistry of supramolecular polymer networks, Chem. Soc. Rev. 41 (2) (2012) 909–930.
[4] S. Chen, W.H. Binder, Dynamic ordering and phase segregation in hydrogen-bonded polymers, Acc. Chem. Res. 49 (7) (2016) 1409–1420.
[5] T. Rossow, S. Hackelbusch, P. van Assenbergh, S. Seiffert, A modular construction kit for supramolecular polymer gels, Polym. Chem. 4 (8) (2013) 2515–2527.
[6] K. Melia, B.W. Greenland, D. Hermida-Merino, L.R. Hart, I.W. Hamley, H.M. Colquhoun, A.T. Slark, W. Hayes, Self-assembling unsymmetrical bis-ureas, React. Funct. Polym. 124 (2018) 156–161.
[7] M. Ahmadi, L.G. Hawke, H. Goldansaz, E. van Ruymbeke, Dynamics of entangled linear supramolecular chains with sticky side groups: Influence of hindered fluctuations, Macromolecules 48 (19) (2015) 7300–7310.
[8] H. Goldansaz, C.-A. Fustin, M. Wübbenhorst, E. van Ruymbeke, How supramolecular assemblies control dynamics of associative polymers: toward a general picture, Macromolecules 49 (5) (2016) 1890–1902.
[9] L. Hawke, M. Ahmadi, H. Goldansaz, E. Van Ruymbeke, Viscoelastic properties of linear associating poly (n-butyl acrylate) chains, J. Rheol. 60 (2) (2016) 297–310.
[10] A. Shabbir, I. Javakhishvili, S. Cerveny, S. Hvilsted, A.L. Skov, O. Hassager, N.J. Alvarez, Linear viscoelastic and dielectric relaxation response of unentangled UPy-based supramolecular networks, Macromolecules 49 (10) (2016) 3899–3910.
[11] R. Larson, Combinatorial rheology of branched polymer melts, Macromolecules 34 (13) (2001) 4556–4571.
[12] A.E. Likhtman, T.C. McLeish, Quantitative theory for linear dynamics of linear entangled polymers, Macromolecules 35 (16) (2002) 6332–6343.
[13] E. Van Ruymbeke, C. Bailly, R. Keunings, D. Vlassopoulos, A general methodology to predict the linear rheology of branched polymers, Macromolecules 39 (18) (2006) 6248–6259.
[14] R. Jongschaap, R. Wientjes, M.H. Duits, J. Mellema, A generalized transient network model for associative polymer networks, Macromolecules 34 (4) (2001) 1031–1038.
[15] M. Rubinstein, A.N. Semenov, Dynamics of entangled solutions of associating polymers, Macromolecules 34 (4) (2001) 1058–1068.
[16] M.E. Shivokhin, M. Narita, L. Talini, A. Habicht, S. Seiffert, T. Indei, J.D. Schieber, Interplay of entanglement and association effects on the dynamics of semidilute solutions of multisticker polymer chains, J. Rheol. 61 (2017).
[17] A. Semenov, M. Rubinstein, Dynamics of entangled associating polymers with large aggregates, Macromolecules 35 (12) (2002) 4821–4837.
[18] W.P. Appel, G. Portale, E. Wisse, P.Y. Dankers, E. Meijer, Aggregation of ureidopyrimidinone supramolecular thermoplastic elastomers into nanofibers: a kinetic analysis, Macromolecules 44 (17) (2011) 6776–6784.
[19] H. Kautz, D. Van Beek, R.P. Sijbesma, E. Meijer, Cooperative end-to-end and lateral hydrogen-bonding motifs in supramolecular thermoplastic elastomers, Macromolecules 39 (13) (2006) 4265–4267.
[20] C. Véchambre, X. Callies, C. Creton, G. Fonteneau, S. Ducouret, L. Pensec, C. Bouteiller, J.-M. Creton, L. Chenal, Chazeau, Microstructure and self-assembly of supramolecular polymers center-functionalized with strong stickers, Macromolecules 48 (22) (2015) 8232–8239.
[21] T. Yan, K. Schröter, F. Herbst, W.H. Binder, T. Thurn-Albrecht, Unveiling the molecular mechanism of self-healing in a telechelic, supramolecular polymer network, Sci. Rep. 6 (2016) 32356.
[22] A. Jangizehi, S.R. Ghaffarian, M. Ahmadi, Dynamics of entangled supramolecular polymer networks in presence of high-order associations of strong hydrogen bonding groups, Polym. Adv. Technol. 29 (2) (2018) 726–735.
[23] A. Jangizehi, S.R. Ghaffarian, W. Schmolke, S. Seiffert, Dominance of chain entanglement over transient sticking on chain dynamics in hydrogen-bonded supramolecular polymer networks in the melt, Macromolecules 51 (8) (2018) 2859–2871.
[24] M. Guo, L.M. Pitet, H.M. Wyss, M. Vos, P.Y. Dankers, E. Meijer, Tough stimuli-responsive supramolecular hydrogels with hydrogen-bonding network junctions, J. Am. Chem. Soc. 136 (19) (2014) 6969–6977.
[25] X. Hu, M. Vatankhah-Varnoosfaderani, J. Zhou, Q. Li, S.S. Sheiko, Weak hydrogen bonding enables hard, strong, tough, and elastic hydrogels, Adv. Mater. 27 (43) (2015) 6899–6905.
[26] Q. Chen, H. Masser, H.-S. Shiau, S. Liang, J. Runt, P.C. Painter, R.H. Colby, Linear viscoelasticity and Fourier transform infrared spectroscopy of polyether–ester–sulfonate copolymer ionomers, Macromolecules 47 (11) (2014) 3635–3644.
[27] Q. Chen, G.J. Tudryn, R.H. Colby, Ionomer dynamics and the sticky rouse model a, J. Rheol. 57 (5) (2013) 1441–1462.
[28] T. Rossow, A. Habicht, S. Seiffert, Relaxation and dynamics in transient polymer model networks, Macromolecules 47 (18) (2014) 6473–6482.
[29] T. Rossow, S. Seiffert, Supramolecular polymer gels with potential model-network structure, Polym. Chem. 5 (8) (2014) 3018–3029.
[30] F.J. Stadler, W. Pyckhout-Hintzen, J.-M. Schumers, C.-A. Fustin, J.-F.O. Gohy, C. Bailly, Linear viscoelastic rheology of moderately entangled telechelic polybutadiene temporary networks, Macromolecules 42 (16) (2009) 6181–6192.
[31] S. Czarnecki, T. Rossow, S. Seiffert, Hybrid polymer-network hydrogels with tunable mechanical response, Polymers 8 (3) (2016) 82.
[32] A. Jangizehi, S.R. Ghaffarian, M. Ahmadi, Dynamics of entangled supramolecular networks in presence of higher order Associations of Ureidopyrimidinone Groups, Polym. Adv. Technol. 29 (2) (2017) 726–735.
[33] A. Pape, M. Bastings, R.E. Kieltyka, H.M. Wyss, I.K. Voets, E. Meijer, P.Y. Dankers, Mesoscale characterization of supramolecular transient networks using SAXS and rheology, Int. J. Mol. Sci. 15 (1) (2014) 1096–1111.
[34] V. Abetz, P.F. Simon, Phase Behaviour and Morphologies of Block Copolymers, Block Copolymers I, Springer, (2005), pp. 125–212.
[35] M. Kossuth, D. Morse, F. Bates, Viscoelastic behavior of cubic phases in block copolymer melts, J. Rheol. 43 (1) (1999) 167–196.
[36] L. Zhang, G. Qiu, F. Liu, X. Liu, S. Mu, Y. Long, Q. Zhao, Y. Liu, H. Gu, Controlled ROMP synthesis of side-chain ferrocene and adamantane-containing diblock copolymer for the construction of redox-responsive micellar carriers, React. Funct. Polym. 132 (2018) 60–73.
[37] G. Qiu, L. Zhao, X. Liu, Q. Zhao, F. Liu, Y. Liu, Y. Liu, H. Gu, ROMP synthesis of benzaldehyde-containing amphiphilic block polynorbornenes used to conjugate drugs for pH-responsive release, React. Funct. Polym. 128 (2018) 1–15.
[38] M.C. Stuparu, A. Khan, C.J. Hawker, Phase separation of supramolecular and dynamic block copolymers, Polym. Chem. 3 (11) (2012) 3033–3044.
[39] S.K. Yang, A.V. Ambade, M. Weck, Main-chain supramolecular block copolymers, Chem. Soc. Rev. 40 (1) (2011) 129–137.
[40] J. Brassinne, J.-P. Bourgeois, C.-A. Fustin, J.-F.O. Gohy, Thermo-responsive properties of metallo-supramolecular block copolymer micellar hydrogels, Soft Matter 10 (17) (2014) 3086–3092.
[41] J. Brassinne, E. Poggi, C.A. Fustin, J.F.O. Gohy, Synthesis and self-assembly of terpyridine end-capped Poly (N-Isopropylacrylamide)-block-Poly (2-(Dimethylamino) ethyl Methacrylate) diblock copolymers, Macromol. Rapid Commun. 36 (7) (2015) 610–615.
[42] J. Brassinne, F. Zhuge, C.-A. Fustin, J.-F.O. Gohy, Precise control over the rheological behavior of associating stimuli-responsive block copolymer gels, Gels 1 (2) (2015) 235–255.
[43] J.R.M. Brassinne, J.-F.O. Gohy, C.-A. Fustin, Controlling the cross-linking density of supramolecular hydrogels formed by heterotelechelic associating copolymers, Macromolecules 47 (13) (2014) 4514–4524.
[44] J.R.M. Brassinne, A.M. Stevens, E. Van Ruymbeke, J.-F.O. Gohy, C.-A. Fustin, Hydrogels with dual relaxation and two-step gel–sol transition from heterotelechelic polymers, Macromolecules 46 (22) (2013) 9134–9143.
[45] L.M. Pitet, A.H. van Loon, E.J. Kramer, C.J. Hawker, E. Meijer, Nanostructured supramolecular block copolymers based on polydimethylsiloxane and polylactide, ACS Macro Lett. 2 (11) (2013) 1006–1010.
[46] K. Yamauchi, J.R. Lizotte, D.M. Hercules, M.J. Vergne, T.E. Long, Combinations of microphase separation and terminal multiple hydrogen bonding in novel macromolecules, J. Am. Chem. Soc. 124 (29) (2002) 8599–8604.
[47] V.F. Scalfani, E.F. Wiesenauer, J.R. Ekblad, J.P. Edwards, D.L. Gin, T.S. Bailey, Morphological phase behavior of poly (RTIL)-containing diblock copolymer melts, Macromolecules 45 (10) (2012) 4262–4276.
[48] C.M. Stancik, A.R. Lavoie, J. Schütz, P.A. Achurra, P. Lindner, A.P. Gast, R.M. Waymouth, Micelles of imidazolium-functionalized polystyrene diblock copolymers investigated with neutron and light scattering, Langmuir 20 (3) (2004) 596–605.
[49] C.-S. Tsao, H.-L. Chen, Concurrent transformation of copolymer domain morphology induced by the order− disorder transition of comb block in supramolecular comb− coil block copolymer, Macromolecules 37 (24) (2004) 8984–8991.
[50] K. Yamauchi, J.R. Lizotte, T.E. Long, Thermoreversible poly (alkyl acrylates) consisting of self-complementary multiple hydrogen bonding, Macromolecules 36 (4) (2003) 1083–1088.
[51] B.J. Folmer, R. Sijbesma, R. Versteegen, J. Van der Rijt, E. Meijer, Supramolecular polymer materials: chain extension of telechelic polymers using a reactive hydrogen-bonding synthon, Adv. Mater. 12 (12) (2000) 874–878.
[52] A. Hammersley, The FIT2D Home Page, ESRF, Grenoble, 2009.
[53] C.J. Gommes, B. Goderis, CONEX, a program for angular calibration and averaging of two-dimensional powder scattering patterns, J. Appl. Crystallogr. 43 (2) (2010) 352–355.
[54] A. Michalski, M. Brzeziński, P. Kubisa, T. Biela, Supramolecular aggregates of linear and star-shaped polylactides with different number of hydroxyl or carboxyl end-groups, React. Funct. Polym. 128 (2018) 67–73.
[55] W. Jakubowski, N.V. Tsarevsky, T. Higashihara, R. Faust, K. Matyjaszewski, Allyl halide (macro) initiators in ATRP: synthesis of block copolymers with polyisobutylene segments, Macromolecules 41 (7) (2008) 2318–2323.
[56] A. Mühlebach, S.G. Gaynor, K. Matyjaszewski, Synthesis of amphiphilic block copolymers by atom transfer radical polymerization (ATRP), Macromolecules 31 (18) (1998) 6046–6052.
[57] D.A. Shipp, J.-L. Wang, K. Matyjaszewski, Synthesis of acrylate and methacrylate block copolymers using atom transfer radical polymerization, Macromolecules 31 (23) (1998) 8005–8008.
[58] K.A. Davis, K. Matyjaszewski, Statistical, Gradient, Block, and Graft Copolymers by Controlled/Living Radical Polymerizations, Statistical, Gradient, Block and Graft Copolymers by Controlled/Living Radical Polymerizations, Springer, (2002), pp. 1–13.
[59] K. Matyjaszewski, D.A. Shipp, G.P. McMurtry, S.G. Gaynor, T. Pakula, Simple and

effective one-pot synthesis of (meth) acrylic block copolymers through atom transfer radical polymerization, J. Polym. Sci., Part A 38 (11) (2000) 2023–2031.
[60] T. Sato, H. Watanabe, K. Osaki, M.-L. Yao, Relaxation of spherical micellar systems of styrene− isoprene diblock copolymers. 1. Linear viscoelastic and dielectric behavior, Macromolecules 29 (11) (1996) 3881–3889.
[61] H. Watanabe, Y. Matsumiya, Rheology of diblock copolymer micellar dispersions having soft cores, Macromolecules 38 (9) (2005) 3808–3819.
[62] M. Ahmadi, S. Pioge, C.-A. Fustin, J.-F. Gohy, E. van Ruymbeke, Closer insight into the structure of moderate to densely branched comb polymers by combining modelling and linear rheological measurements, Soft Matter 13 (5) (2017) 1063–1073.
[63] M. Entezam, M. Abbasi, M. Ahmadi, Theoretical correlation of linear and non-linear rheological symptoms of long-chain branching in polyethylenes irradiated by electron beam at relatively low doses, Rheol. Acta 56 (9) (2017) 729–742.
[64] E. Van Ruymbeke, C.-Y. Liu, C. Bailly, Quantitative tube model predictions for the linear viscoelasticity of linear polymers, Rheol. Rev. (2007) 53–134.
[65] E. Van Ruymbeke, R. Keunings, C. Bailly, Prediction of linear viscoelastic properties for polydisperse mixtures of entangled star and linear polymers: modified tube-based model and comparison with experimental results, J. Non-Newtonian Fluid Mech. 128 (1) (2005) 7–22.
[66] M. Ahmadi, C. Bailly, R. Keunings, M. Nekoomanesh, H. Arabi, E. van Ruymbeke, Time marching algorithm for predicting the linear rheology of monodisperse comb polymer melts, Macromolecules 44 (3) (2011) 647–659.
[67] K.E. Feldman, M.J. Kade, E. Meijer, C.J. Hawker, E.J. Kramer, Model transient networks from strongly hydrogen-bonded polymers, Macromolecules 42 (22) (2009) 9072–9081.
[68] M. Beiner, H. Huth, Nanophase separation and hindered glass transition in side-chain polymers, Nat. Mater. 2 (9) (2003) 595–599.
[69] L. Bosio, G. Johari, M. Oumezzine, J. Teixeira, X-ray and neutron scattering studies of the structure of water in a hydrogel, Chem. Phys. Lett. 188 (1–2) (1992) 113–118.
[70] Y. Liu, H. Nie, R. Bansil, M. Steinhart, J. Bang, T.P. Lodge, Kinetics of disorder-to-fcc phase transition via an intermediate bcc state, Phys. Rev. E 73 (6) (2006) 061803.